Frontiers in Bioscience Landmark

Front. Biosci. (Landmark Ed) **2026**; 31(2): 47298
https://doi.org/10.31083/FBL47298

Original Research

A Self-Assembled Nanobody Against the Haemagglutinin of Influenza a Virus Shows Enhanced Stability and Efficacy *In Vitro* and *In Vivo*

Qian Weng[1,†], Honggang Liu[1,†], Xue Yan[1], Cheng Xu[1], Qin Wang[1], Yifan Xu[1], Junwei Li[1,2,3,*]

[1]Department of Infectious Disease, The Second Hospital of Nanjing, Affiliated with Nanjing University of Chinese Medicine, 210003 Nanjing, Jiangsu, China
[2]Medical Innovation Center for Infectious Disease of Jiangsu Province, 210003 Nanjing, Jiangsu, China
[3]College of Veterinary Medicine, Qingdao Agricultural University, 266109 Qingdao, Shandong, China
*Correspondence: junwli@yeah.net (Junwei Li)
[†]These authors contributed equally.

Academic Editor: Graham Pawelec
Submitted: 13 October 2025 Revised: 14 January 2026 Accepted: 19 January 2026 Published: 10 February 2026

Abstract

Background: In recent years, drug-resistant influenza viruses have emerged frequently, making influenza a persistent and serious public health burden. Therefore, potential anti-influenza virus drugs are urgently needed. Nanobodies, variable domains of heavy-chain antibodies (VHHs), have the advantages of easy preparation, excellent solubility, deep tissue penetration, and weak immunogenicity; thus, they have broad application prospects in the fields of basic research and drug development. However, its short half-life and low stability limit its clinical therapeutic application. Fenobody is an engineered display platform with the ability to present multimerized nanobodies on the surface of ferritin to overcome these disadvantages and increase its potency. **Methods**: In this study, we engineered a fenobody displaying multimerized VHH against haemagglutinin (HA) of influenza virus (A/California/07/2009(H1N1), pdm09) on the surface of ferritin by using the property of SpyTag to spontaneously bind to SpyCatcher, named ferritin-NP-VHH. **Results**: Compared with VHH alone, ferritin-NP-VHH improved the cross-neutralizing activity, stability and affinity for influenza virus *in vitro* and prolonged its half-life *in vivo*. **Conclusions**: These results suggest that the implementation of genetic engineering technology to construct multimerized anti-influenza virus nanoparticles provides new tools to control infection with influenza virus.

Keywords: fenobody; nanobody; influenza virus; stability; affinity; protection

1. Introduction

Influenza is an important human respiratory infectious disease caused by seasonal or emerging influenza viruses. Statistically, infection by seasonal influenza viruses kills 250,000–500,000 people worldwide each year [1–3]. In recent years, drug-resistant strains and new subtypes of influenza viruses that infect humans have emerged frequently, making infection with influenza virus a persistent and serious public health problem [4–7]. Although vaccination is the primary method for preventing infection by the influenza virus, its implementation poses some technical challenges. These include (i) difficulty in predicting which strains will emerge and infect humans in the coming season, (ii) the lag period between the emergence of new strains and the availability of clinically approved vaccines, and (iii) poor immune response in aged and immunocompromised people [8,9]. Therefore, given the increase in drug resistance, reduced vaccination effectiveness in some populations, and the short therapeutic window of existing antiviral drugs, a new type of anti-influenza virus is urgently needed [10,11].

Nanobodies, also known as VHHs, are the variable domain of heavy-chain immunoglobulins (HcAbs) found in the family Camelidae. Despite their small size (12–15 kDa), VHHs are superior to conventional antibodies in terms of affinity and specificity [12–14]. Owing to their exceptional stability over a wide temperature range, resistance to the action of various detergents, and proteolytic cleavage, single-domain antibodies can be delivered into the body orally and by inhalation [15–19]. However, the samll size render nanobodies with short serum half-life and low affinity, that limits its therapeutic application *in vivo*.

Ferritin [20–22] is an important functional protein that regulates the storage and release of iron. Naturally, synthesized ferritin mostly presents a hollow spherical nanocage structure with an outer diameter of 12 nm and an inner diameter of 8 nm. Its spherical structure consists of an inner core and an outer shell. The inner core is mainly full of minerals. When ferritin is used as a nanocarrier, the target molecule can be wrapped inside the cage to be released slowly, or the target molecule can be anchored on the outer surface of the cage to stabilize the structure and efficiently deliver the target protein. Moreover, ferritin is easily produced in E. coli at high yield and resistant to high temperature and various detergents because of its high stability and exhibits excellent biocompatibility, without affecting its natural structure

[23]. Therefore, self-assembled ferritin nanoparticles have recently been widely applied in drug delivery [24–26].

In the current study, we rationally designed a ferritin particle-based multimeric VHH, named fenobody. We linked VHH, an anti-haemagglutinin of an influenza virus nanobody, to the C-terminus of the ferritin monomer subunit for fusion expression, thereby anchoring the VHHs on the surface of the self-assembled ferritin nanocages. This ferritin particle-based multimeric nanobody was named ferritin-NP-VHH. Our *in vitro* and *in vivo* results suggest that compared with monovalent VHH, ferritin-NP-VHH has impressive prevention and therapeutic effects against the infection by influenza virus.

2. Materials and Methods

2.1 Influenza a Virus, Cells, and Mice

A/Puerto Rico/8/1934 (PR8, H1N1) was preserved by the Laboratory of Preventive Veterinary Medicine, Qingdao Agricultural University. CHO cells (CHO-2H6) lacking the GS gene and MDCK cells (ATCC, CRL-2936) were preserved in the Second Hospital of Nanjing affiliated the University of Chinese Medicine. CHO-2H6 cells were cultured in CHOGrow®302 medium purchased from Yuanpei (Shanghai) Biotechology Co., Ltd. MDCK cells were cultured in DMEM medium supplemented with 10% fetal bovine serum (FBS) and 10 units/mL of penicillin and 10 µg/mL of streptomycin. All cells were maintained at 37 °C and 5% CO_2 atmosphere. All cell lines were validated by short tandem repeats (STR) profiling and tested negative for mycoplasma. 6 to 8 week-old female specific pathogen-free (SPF) BALB/c mice were purchased from Jinan Pengyue (Jinan) Experimental Animal Breeding Co., Ltd., and raised at the Animal Breeding Center of Qingdao Agricultural University with a germ-free environment.

2.2 Cloning, Expression and Purification of Fusion Proteins

The genes encoding SpyTag-ferritin and SpyCatcher-VHH were synthesized by GenScript (Nanjing) and optimized with CHO preferred codons. Ferritin is adopted from residues 5–174 of Pf ferritin. VHH (R1a-G6) was reported by Simon E. Hufton and colleagues [9]. Three G3S linkers were inserted between SpyTag and Ferritin and between SpyCatcher and VHH. His-tag was added at the carboxy terminus of SpyCatcher-VHH. The amino terminus of the SpyTag-ferritin and SpyCatcher-VHH genes followed after a murine IgG signal peptide sequence. The DNA sequence of the signal peptide is 5′-GAATTCATGGGTTGGAGTTGCATCATCCTATTTCTAGTGGCCACCGCTACCGGCGTG. Subsequently, the SpyTag–ferritin and SpyCatcher-VHH gene segments were amplified and inserted into the P3 plasmid containing the GS gene between the XbaI and Hind III sites. The successfully cloned P3 plasmid was introduced into GS gene-deficient CHO cells by electroporation. The procedure is set as follows. After being digested, the eukaryotic expression plasmids, 20 µg P3-SpyTag-Ferritin and 20 µg P3-Spy Catcher-VHH respectively, were added into the resuspended CHO-2H6 suspension cell culture and gently mixed, then the cells were incubated at room temperature for 10 minutes. Electroporator (ECM830) parameter (Holliston, MA, USA) is voltage 280 V, time 20 ms. Mixture of plasmids and CHO cells were added into a precooled 4 mm cuvette and electroporation was conducted, then the mixture was transferred into a culture flask preheated to 37 °C, with serum-free CHOGrow®302 medium containing L-alpha-aminoglutamic acid. After 24-hour static culture, the cells were transferred into a 125 mL cell culture flask, and suspended in vertical shaking incubator at 37 °C, 5% CO_2, with speed of 110 rpm. During cell culture, number counting and viability test are performed every 24 hours, then viable cells were frozen for further use.

The CHO cells stably carrying P3-SpyTag-Ferritin or P3-SpyCatcher-VHH were screened by using medium without L-glutamine. After the screening was completed, the CHO cells were continuously cultured, and supernatant was collected for protein purification when the cell viability reached 70%. SpyTag-ferritin were purified using a Superose 6 Increase (GE Healthcare, Wauwatosa, WI, USA) size exclusion column according to the manufacturer's protocol. SpyCatcher-VHH was purified using a Ni-NTA agarose column (Thermo Fisher Scientific, Shanghai, China) according to the manufacturer's protocol.

2.3 Preparation and Purification of Ferritin-NP-VHH

SpyTag-ferritin and SpyCatcher-VHH were mixed at a 1:1 molar ratio and incubated overnight at 4 °C. Ferritin-NP-VHH was then purified using a Superose 6 Increase size exclusion column. Impurities were removed by using a 220 nm filter prior to purify ferritin-NP-VHH.

2.4 Negative-Stain Electron Microscopy

5 µL purified sample was dropped on a 300-mesh carbon-supported membrane copper grid and stained with 2% (w/v) uranyl acetate. Excessive uranyl acetate was removed until the copper mesh was dry. The sample was then observed under a transmission electron microscope (Hitachi, Tokyo, Japan) at a scale of 100 nm.

2.5 Enzyme-Linked Immunosorbent Assay (ELISA)

Ferritin-NP-VHH and monovalent VHH were tested for their avidity with H1N1 influenza virus by indirect ELISA. ELISA plates were coated with H1N1 influenza virus at 200 ng/well and incubated overnight at 4 °C. Afterwards, the plates were washed three times with 300 µL PBST and blocked in 300 µL of 2.5% nonfat milk at 37 °C for 2 hours. After the plate was washed three times with 300 µL PBST, 400 ng of ferritin-NP-VHH or monovalent VHH was added into each well, and the plate was incubated at 37 °C for 1 hour. After three-times wash with 300 µL PBST in

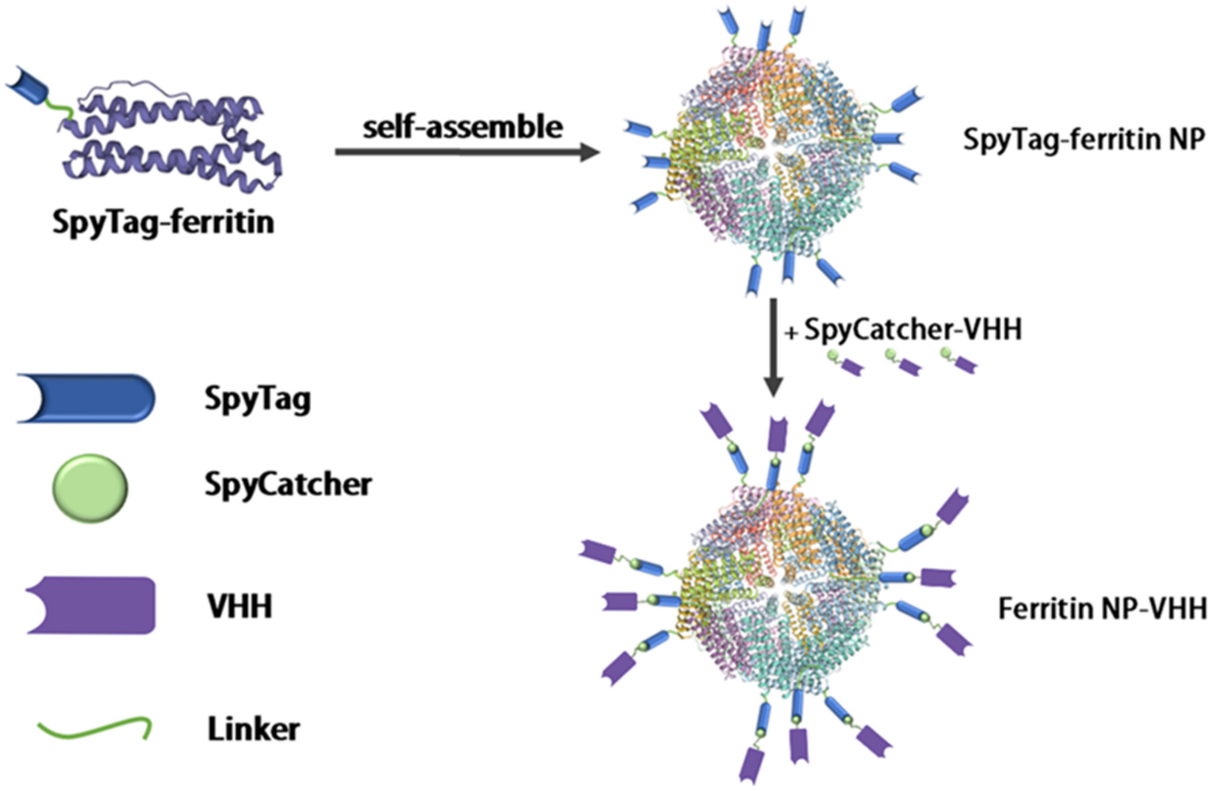

Fig. 1. Design of the multimerization of nanobodies. Using modified SpyTag/SpyCatcher technology, the VHH was exposed to the outer surface of the ferritin shell. Each ferritin is composed of 24 ferritin monomers, and 24 VHHs can be displayed on the surface of each ferritin particle to form anti-influenza virus nanoparticles, thereby realizing the multimerization of nanobodies. VHH, variable domains of heavy-chain antibody.

each well, the plates were incubated at 37 °C for 1 hour and 100 µL of mouse anti-His polyclonal antibody (66005-1-lg, Proteintech, Wuhan, China) diluted 1:2000 was added into each well. After three-times wash, 100 µL of 1:5000 diluted goat anti-mouse-HRP-labelled antibody (SA00001-1, Proteintech) was added into each well, and the plate was incubated at 37 °C for 1 hour. After being washed, the plate was incubated with 100 µL of chromogenic solution per well for 15 minutes at room temperature in the dark. Finally, the reaction was terminated with 50 µL of 2 M H_2SO_4 per well, and the OD_{450nm} was read in an automatic microplate reader (BioTek, Winooski, VT, USA).

For comparing the affinity of ferritin-NP-VHH or monovalent VHH with H1N1 influenza virions, plates were coated with 800 ng of ferritin-NP-VHH or monovalent VHH per well and incubated at 4 °C overnight. After being washed with 300 µL PBST, plates were blocked with 300 µL/well of 2.5% non-fat milk at 37 °C for 2 hours, the plates were washed three times with 300 µL PBST again. Then, 100 µL of H1N1 influenza virions diluted in gradient dilutions was added into each well, and the plates were incubated at 37 °C for 2 hours. After the plate was washed three times, 100 µL of 1:2000 diluted H1N1 HA mAb (11085-MM01, SinoBiological, Beijing, China) was added into each well, and the plates were incubated at 37 °C for 1 hour. After the plate was washed three times, 100 µL of 1:5000 diluted goat anti-mouse-HRP was added into each well, and the plate was incubated at 37 °C for 1 hour. After the plate was washed three times with 100 µL of chromogenic solution per well, the plates were incubated at room temperature for 15 minutes in the dark. Finally, the reaction was stopped with 50 µL of 2 M H_2SO_4 in each well, and the plates were read at an OD_{450nm} in a plate reader. The binding constant Kd of the binding reaction was accurately calculated by using GraphPad Prism software (GraphPad Software, Boston, MA, USA, version 5.0).

2.6 Analysis of the Neutralizing Activity of Ferritin-NP-VHH and Monovalent VHH for Influenza Virus

5×10^4 cells MDCK cells were seeded into 24-well plates per well. Ferritin-NP-VHH or monovalent VHH (0.1 µg, 1 µg, 10 µg, or 50 µg) was mixed with 5×10^4 PFU of influenza virus and allowed to stand at room temperature for 15 minutes. The mixture was added to each well, with 5 replicates in each group. After being incubated for 48 hours at 37 °C, the supernatant in each well was collected. A standard plaque assay was used to determine the viral titres and plaque size in each well.

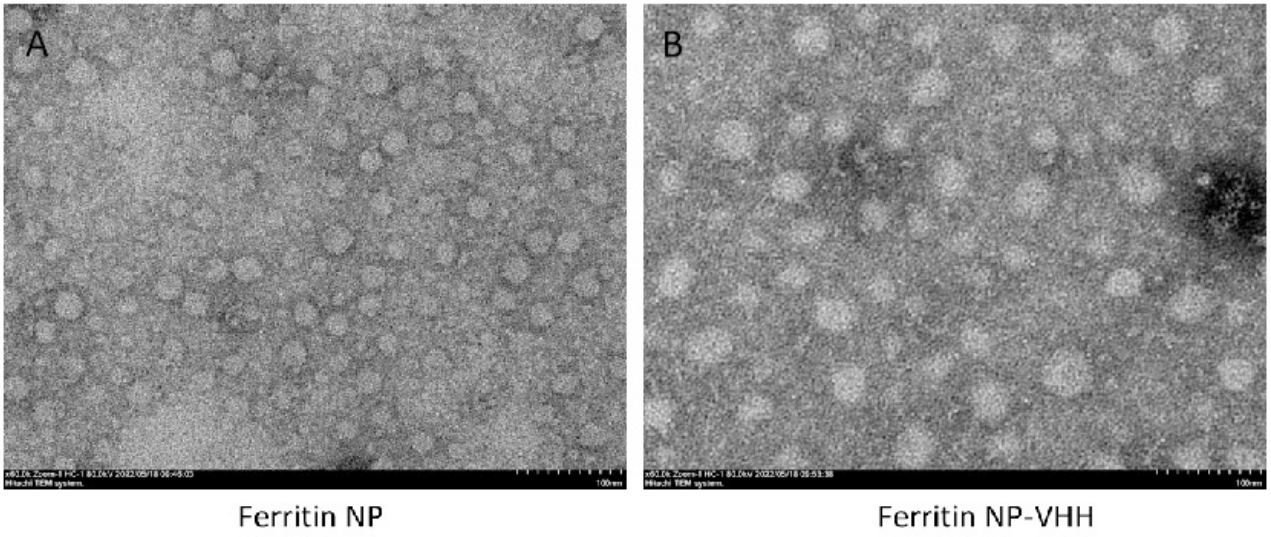

Fig. 2. Images of ferritin particle (A) and ferritin-NP-VHH (B) were taken by transmission electron microscopy. Under the same magnification conditions, the particle size of ferritin-NP-VHH is significantly larger than that of ferritin particle. NP, nanoparticle. Scale bar = 100 nm.

2.7 Half-Life Assay

Ferritin-NP-VHH and monovalent VHH were placed in dialysis bags containing carbonate buffer (CBS) and dialyzed at 4 °C for 24 hours. Then, 200 nM FITC and 50 nM Ferritin-NP-VHH or monovalent VHH were incubated overnight at 4 °C with rotation to label Ferritin-NP-VHH and VHH, then the mixture was dialyzed in CBS at 4 °C with stirring for 24 hours to remove the surplus FITC. The dialysate was transferred from the dialysis bag into an ultrafiltration tube and centrifuged at 4000 rpm at 4 °C. Subsequently, equal amounts (50 µg) of FITC-labelled ferritin-NP-VHH or monovalent VHH were injected into female BALB/c mice via the tail vein. Blood was collected from the submandibular vein at different time points, and the fluorescence value of the FITC-labelled protein in the blood was measured at an excitation wavelength of 485 nm and an emission wavelength of 535 nm on a VICTOR™ X series multi-label microplate reader (Waltham, MA, USA).

2.8 Challenge Experiments With Influenza Virus in Mice

All experiments were approved by the Animal Ethics Committee of Qingdao Agricultural University and performed according to the committee's guidelines. Female BALB/c mice (6–8 week-old) were randomly divided into groups of each group with 8 mice and housed under designated pathogen-free conditions with food and water ad libitum. Before administration and challenge, mice were anaesthetized with isoflurane. All steps are performed in a biosafety hood equipped with a charcoal filter, including (1) prepare mixture of 20%v/v isoflurane in propylene glycol, (2) soak cotton pad in the mixed isoflurane, (3) retrieve mouse nose close to the soaked cotton with isoflurane mixture. The depth of anesthesia can be adjusted by moving the nostrils closer to or farther from the cotton pad, and then intranasally administered 50 µg ferritin-NP-VHH or monovalent VHH at 4 hours before and 24 hours after challenge with $2\times LD_{50}$ influenza virus A/Puerto Rico/8/1934 (H1N1). A group treated with PBS was used as a native control. Body weight and survival rate were continuously monitored for 14 days. Humane endpoints were applied when weigh loss is greater than 25%. To determine the pathological changes and viral titres in the lung tissue of mice treated with ferritin–NP-VHH or monovalent VHH, another independent experiment was performed. On the 3rd day after infection with influenza virus A/Puerto Rico/8/1934 (H1N1), following deep euthanasia in accordance with institutional animal care guidelines, mouse cervical dislocation was performed, then tissues were dissected under sterile and controlled conditions. For lung sample collection, the thoracic cavity was opened, then the lungs were removed, and peripheral tissue was dissected from the lower lobes while avoiding major airways to ensure comparable sampling across animals. Next, whole lung samples were sent to Servicebio to perform H&E staining for pathological change testing in lung tissue or viral replication by testing the concentration of the N gene segment by RT-PCR.

2.9 Hematoxylin and Eosin Staining

Lung specimens were collected, fixed in 10% neutral buffered formalin, and embedded in paraffin wax. Five-micrometer-thick sections were stained with hematoxylin and eosin (H&E) and evaluated for histopathological alterations.

2.10 RNA Analysis

Lung samples of mice were collected and total RNA was extracted by using an RNeasy RNA extraction kit (Qiagen, Düsseldorf, Germany) according to the manufacturer's protocol. The concentration of viral RNAs (vRNAs) was quantified by real-time RT-PCR with primers specific for the NP gene which was conducted in two steps by using a SuperScript III Platinum two-step qRT-PCR kit with SYBR green (Invitrogen, Carlsbad, CA, USA) as per the manufacturer's instructions in an iCycler iQ-Multicolor real-time PCR detection system (Bio-Rad, Hercules, CA, USA). Specifically, vRNA was reverse-transcribed by using the Uni-12 primer and amplified by PCR using F5′-GATTGGTGGAATTGGACGAT and B5′-AGAGCACCATTCTCTCTATT as primers. The concentrations of vRNA were obtained by comparison with serially diluted plasmid carrying NP gene segment. All RNA determinations were assayed in duplicate and repeated three times.

2.11 Statistical Analysis

Comparisons between different groups were performed by using nonparametric one-way ANOVA with the Tukey multiple comparison test and Fisher's exact test. The survival data were analysed by using log-rank test. All analyses were performed by using GraphPad Prism version 5.0 for Windows (GraphPad Software). p values < 0.05 were considered to be significant.

3. Results

3.1 Specific Affinity Analysis of Ferritin-NP-VHH and Influenza Virus

In this study, ferritin-NP-VHH was generated using a modified SpyTag/SpyCatcher technique in which VHH was linked at the C-terminal of SpyCatcher convalently, as shown in Fig. 1 [27–30]. Both SpyTag-ferritin and SpyCatcher-VHH were expressed in glutamine synthetase (GS)-deficient CHO cells [31–35]. The self-assembled nanoparticles were confirmed by transmission electron microscopy (TEM), and the particle size of Ferritin–NP-VHH was slightly larger than that of SpyTag-ferritin, as shown in Fig. 2.

To evaluate the specific binding activity of ferritin-NP-VHH, monovalent VHH with influenza virus, ELISA plates were coated with H1N1 influenza virus overnight, after which equivalent amounts (0.03 µM each) of ferritin-NP-VHH or monovalent VHH were added to each well. The plates were read in a plate reader at an absorbance of 450 nm. Finally, the data were analysed by using GraphPad Prism software (version 5.0), and the binding constant Kd was calculated. The results showed that both ferritin-NP-VHH and monovalent VHH are efficiently bound to the influenza virus. However, compared with monovalent VHH, ferritin-NP-VHH was more sensitive to influenza virus capture by 7.18-fold, as shown in Fig. 3.

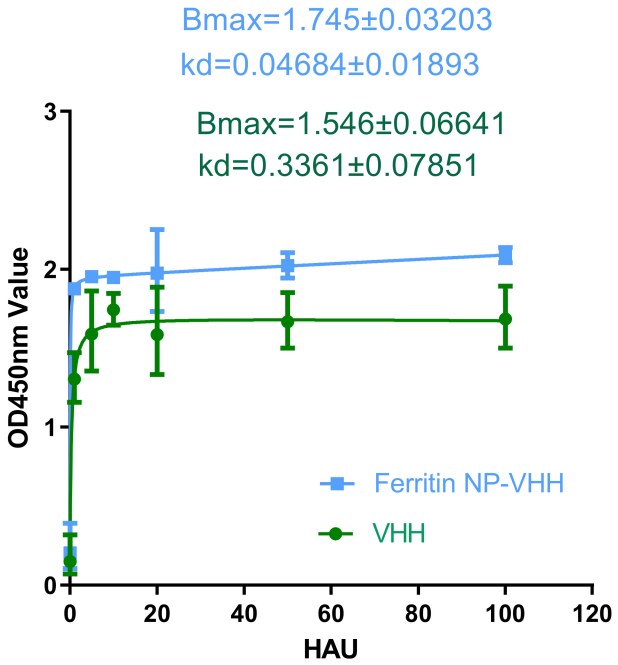

Fig. 3. Binding of ferritin-NP-VHH or monomer VHH with influenza virus. Both ferritin-NP-VHH and VHH can specifically bind to influenza virus, but the capture affinity of ferritin-NP-VHH (Kd = 0.4684 ± 0.01893 HAU/mL) for the virus is 7.18 times greater than that of the monomer VHH (3.361 ± 0.07851 HAU/mL) (Error bars represent SD).

3.2 Analysis of Specific Neutralizing Activity

Next, we determined the specific neutralizing activity of ferritin-NP-VHH or monovalent VHH with influenza virus by using the standard plaque assay method. The neutralization and plaque size results show that ferritin-NP-VHH conferred higher neutralizing activity than monovalent VHH against the influenza virus, as shown in Fig. 4A,B.

3.3 Analysis of the Half-Life of Ferritin-NP-VHH Particles in Mouse Blood

To compare the half-life of ferritin-NP-VHH with that of monovalent VHH *in vivo*, the fluorescence values in the blood of BABL/c mice injected with ferritin-NP-VHH-FITC or monovalent VHH-FITC by tail vein were measured. The results show that the half-life of ferritin-NP-VHH in the blood is 2.44 times longer than that of monovalent VHH, as shown in Fig. 5.

3.4 Protection of Mice Against Lethal Influenza a Virus Challenge by Intranasal Administration of Ferritin-NP-VHH

We subsequently investigated the protective potential of ferritin-NP-VHH against lethal infection with influenza A virus *in vivo*. Eight-week-old female BALB/c mice were inhaled intranasally with 50 µg ferritin-NP-VHH

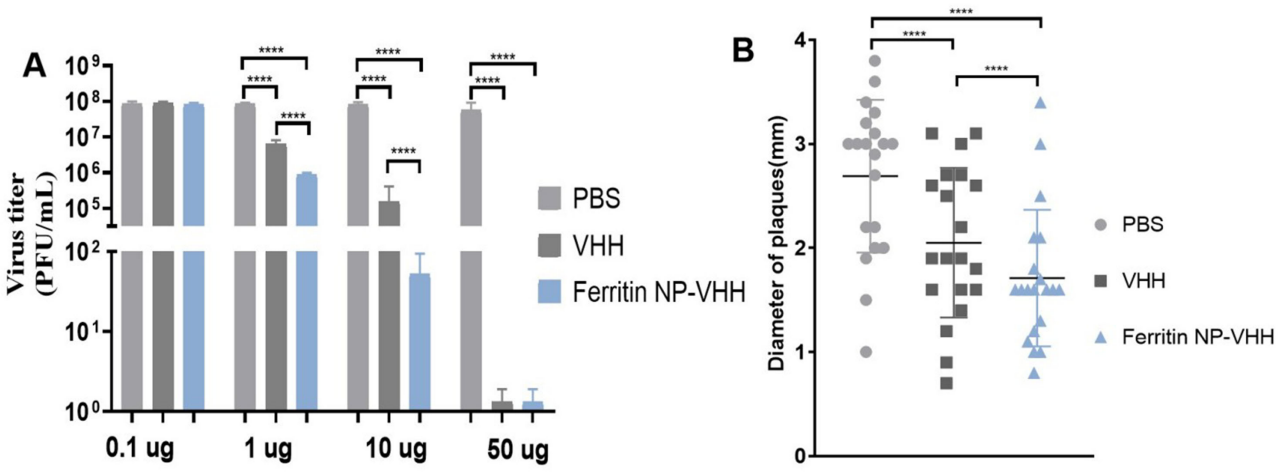

Fig. 4. Neutralization of ferritin-NP-VHH or monomer VHH with influenza virus. Both ferritin-NP-VHH and VHH showed potent neutralizing activity against influenza virus. However, neutralization (A) and plaque size (B) suggested ferritin-NP-VHH conferred higher neutralizing activity against influenza virus than monomeric VHH (SD was specified as error bars and ****p value $<$0.0001).

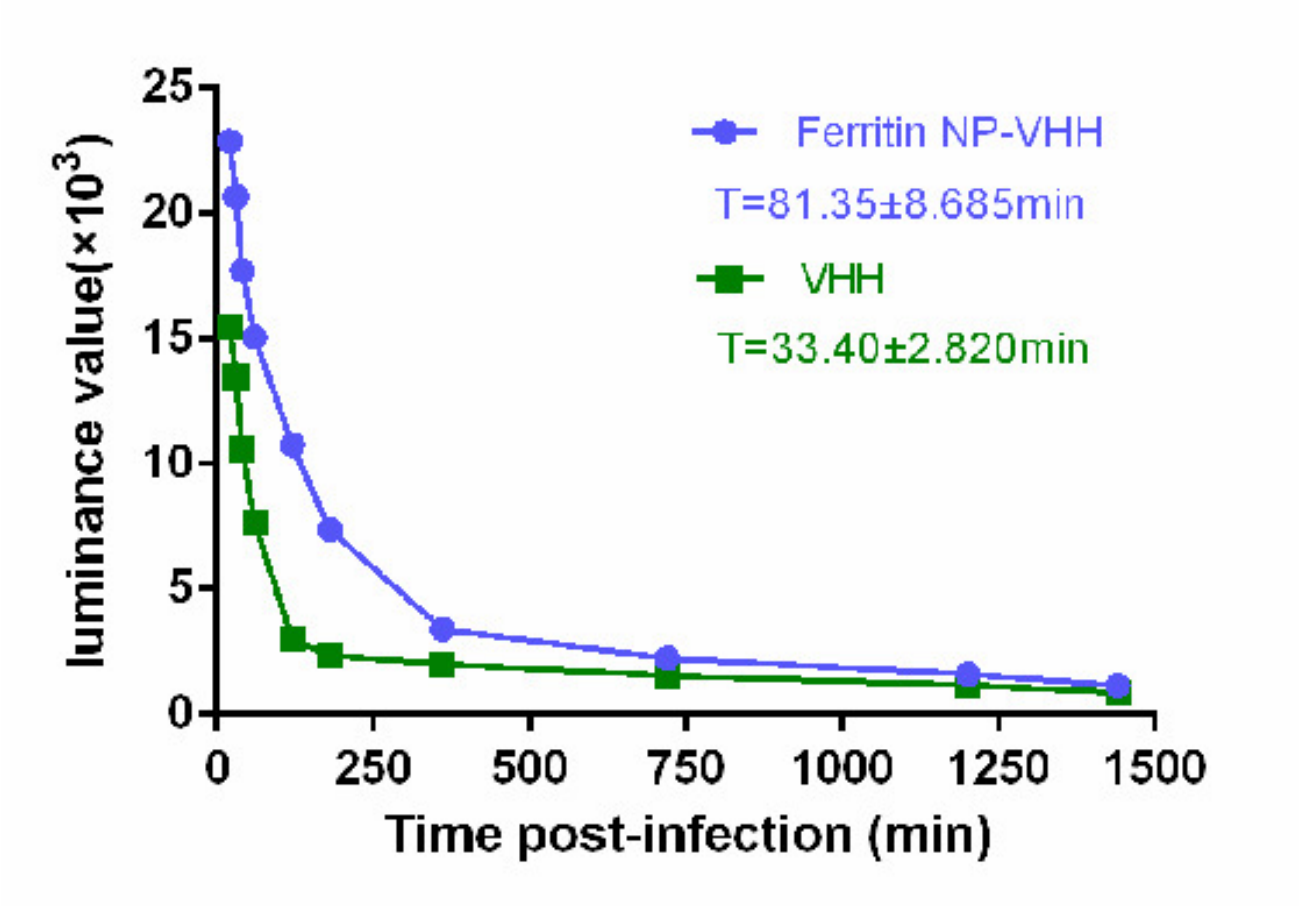

Fig. 5. Ferritin-NP-VHH had a longer half-life than mononer VHH did in mice. To compare the half-lives of ferritin-NP-VHH and VHH, the fluorescence values in the blood of BABL/c mice injected with ferritin-NP-VHH/VHH-FITC were measured. The results show that the half-life of ferritin-NP-VHH in the blood is approximately 2.44 times longer than that of VHH. FITC, fluorescin isothiocyanate.

or 50 μg monovalent VHH at 4 hours before and 24 hours after challenge with the influenza A/Puerto Rico/8/1934 (H1N1) virus at a dose of $2\times LD_{50}$. In the control group, the mice were treated with PBS. The results revealed that

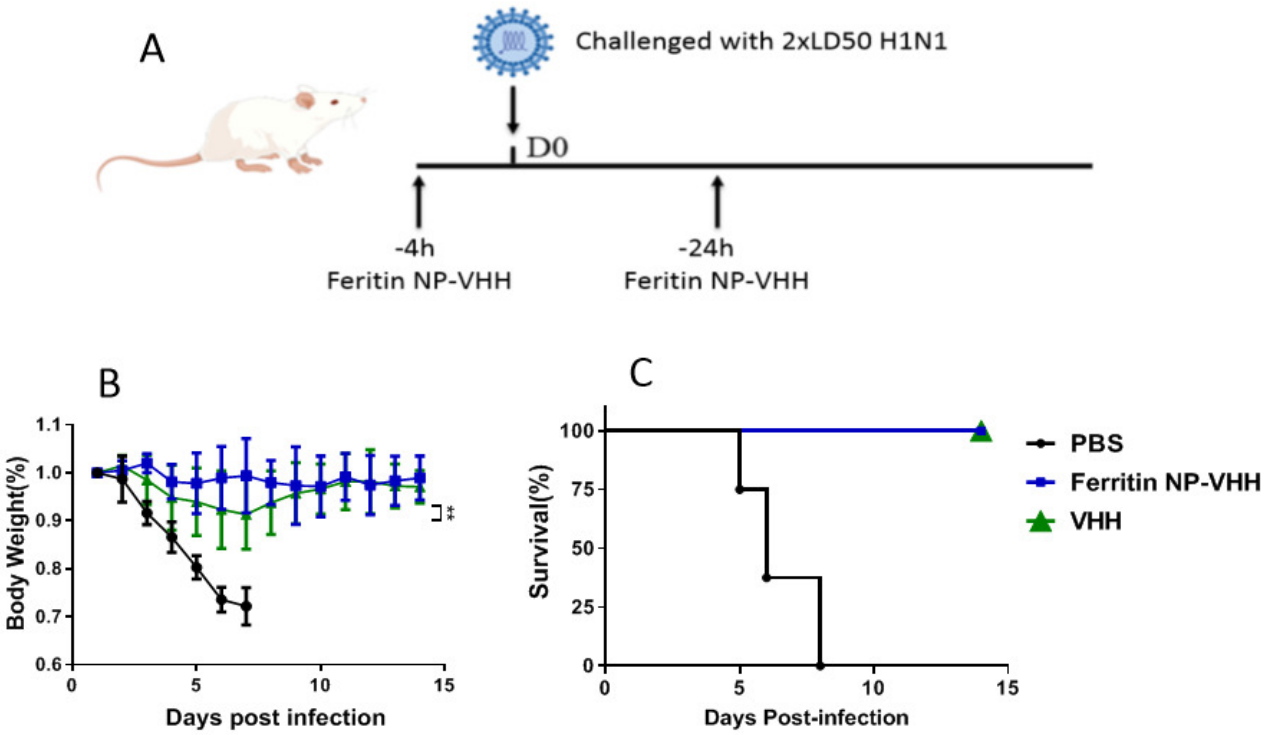

Fig. 6. Ferritin-NP-VHH and monomeric VHH provided protection for mice against challenge with lethal influenza virus. Compared with PBS control mice, mice treated with ferritin-NP-VHH were significantly better protected, as indicated by weight loss and lethality caused by influenza virus infection. Furthermore, compared with mice in the VHH group, mice in the ferritin-NP-VHH group had significantly less body weights after the challenge (n = 8 SD was specified as error bars, $^{**}p < 0.01$). (A) Flowchart illustrating the schedule of animal experiments. (B) Changes in the body weight of mice following A/PR/8/34 (H1N1) challenge. (C) The survival rate of mice post-H1N1 challenge. PBS, phosphate buffer saline.

mice treated with ferritin-NP-VHH had significantly less weight loss and a higher survival rate than mice treated with PBS control or monovalent VHH did, as shown in Fig. 6. Moreover, significantly greater body weight loss after challenge with influenza virus was observed in the monovalent VHH group than in the ferritin-NP-VHH group on Day 6 ($p < 0.01$). These findings suggest that ferritin-NP-VHH provides potential protection against lethal infection with influenza viruses in mice.

Additionally, pathological changes were detected in the lungs of mice challenged with the influenza A/Puerto Rico/8/1934 (H1N1) virus. Significant histological changes, such as diffuse inflammation of the interalveolar septa accompanied by intra-alveolar oedema, were observed in the lung sections of mice in the PBS group; otherwise, few pathological changes and less viral replication were observed in the lung tissues of mice in the ferritin-NP-VHH group (Fig. 7A–C). The NP gene segment was presented in a very low level (Fig. 7D). These findings indicated that ferritin-NP-VHH protected mice from infection by the influenza A/Puerto Rico/8/1934 (H1N1) virus.

4. Discussion

Engineered VHH fragments have enhanced specificity, activity, half-life, and cross-protection for the prevention or treatment of infectious diseases [36,37]. Here, we displayed VHH fragments against the HA of the influenza virus (A/California/07/2009(H1N1) pdm09) on the surface of ferritin particles to obtain multimeric nanoparticles and tested whether compared with VHH monomers, VHH improved the activity of anti-influenza virus. To explore this possibility, both SpyTag-ferritin and SpyCatcher-VHH were expressed in GS-deficient CHO cells by using modified SpyTag/SpyCatcher technology. The two proteins were then linked by using the automatic linking property of SpyTag and SpyCatcher to obtain multimeric nanoparticles on the basis of the ferritin platform.

The assembled ferritin-NP-VHH particles and SpyTag-ferritin particles were observed under the same conditions by TEM. The particles of ferritin-NP-VHH were significantly larger than those of SpyTag-ferritin particles were, indicating that SpyTag-ferritin and monovalent VHH were assembled successfully to fix multimerized nanoparticles. We first tested the half-life of ferritin-NP-VHH and monovalent VHH in mice. The half-life

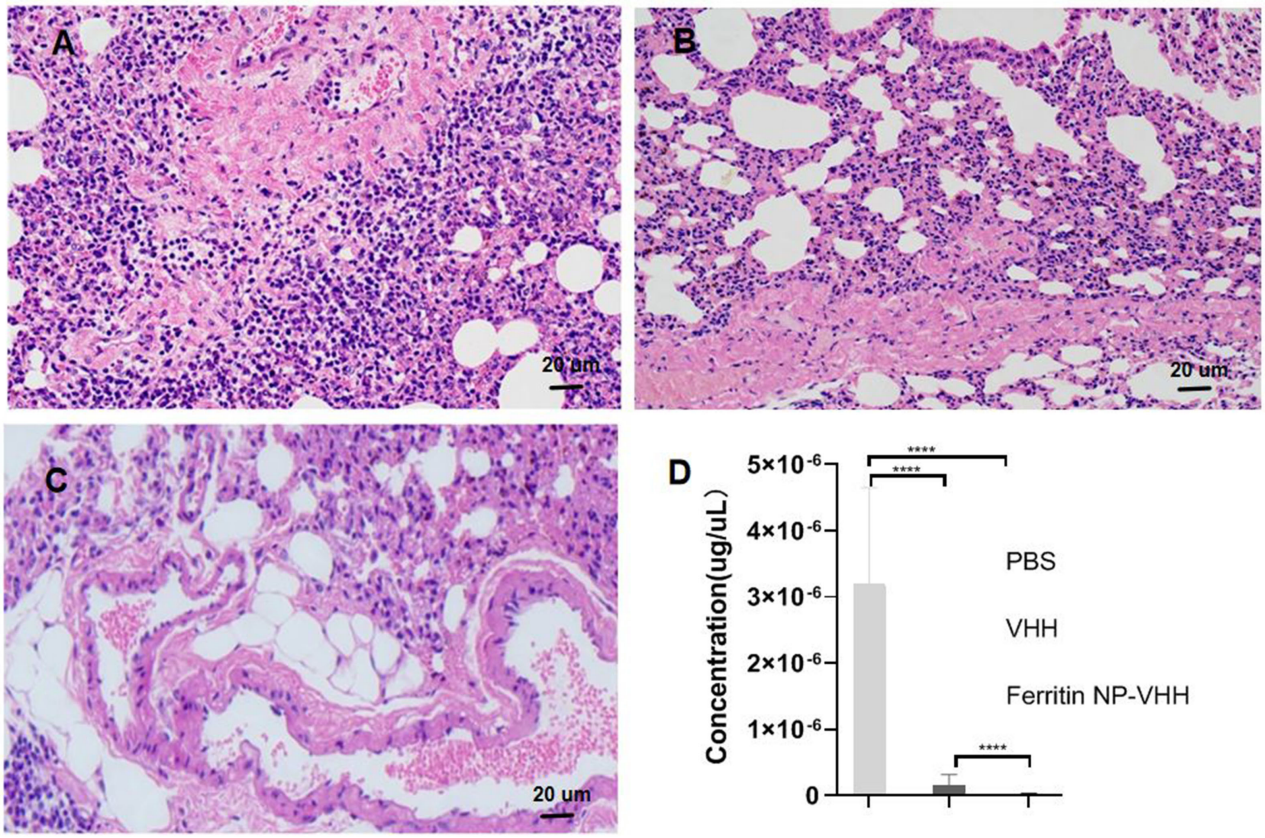

Fig. 7. Pathological alterations in the lungs of mice. Pathological alterations in each tissue section were examined via microscopy at an original magnification of 40×. (A) PBS group, (B) VHH group, (C) ferritin-NP-VHH group. The results showed that ferritin-NP-VHH and VHH reduced the infiltration of inflammatory cells, improved the widening of alveolar septa, and reduced serous exudate, and ferritin-NP-VHH conferred slightly better protection than VHH did. (D) Concentrations of the NP gene segment (n = 8 and SD was specified as error bars, ****p value < 0.0001). Scale bar = 20 μm.

of ferritin-NP-VHH was longer than that of monovalent VHH. We evaluated the specific binding activity and sensitivity of ferritin-NP-VHH and monovalent VHH to A/Puerto Rico/8/1934 (H1N1) influenza virus. We found that the specific binding activity and sensitivity of ferritin-NP-VHH to influenza virus were significantly greater than those of monovalent VHH. Similar results have been presented by other researchers. Wang *et al.* [38] reported the construction of a Salmonella-specific fenobody through the fusion of a nanobody to ferritin, resulting in a self-assembled 24-valent nanocage-like structure. Compared with the conventional nanobody, their fenobody exhibited a 35-fold increase in avidity while retaining good thermostability and specificity. Next, we verified the neutralizing activity of ferritin-NP-VHH and monovalent VHH with influenza, and both had neutralizing activity with A/Puerto Rico/8/1934 (H1N1) influenza virus. Fan and colleagues [39] also reported that the half-life of fenobody was 10-fold longer than that of its monomer counterpart in a murine model and that antibody binding increased approximately 360-fold when H5N1 fenobody was used. Fenobodies can also be self-assembled in silkworm baculovirus expression systems, and ferritin self-assembly technology can effectively increase the neutralization activity of nanobodies against SARS-CoV-2 [40,41]. Wang and colleagues [38] reported that fenobody increased the specific neutralizing activity against hepatitis E virus capsid and provided broad protection.

Finally, we compared ferritin-NP-VHH and monovalent VHH in protecting mice against potentially lethal influenza A virus challenge. Mice treated with ferritin-NP-VHH particles conferred significant protection against lethal infection by A/Puerto Rico/8/1934 (H1N1) influenza virus, as indicated by weight loss and survival rate. These findings suggested that the preventive and therapeutic function of ferritin-NP-VHH particles was significantly better than that of monovalent VHH.

In this study, our results showed that ferritin-NP-VHH provided superior neutralization and protection against A/Puerto Rico/8/1934 (H1N1) influenza virus although the original VHH (R1a-G6) was selected against influenza virus A/California/7/09 (H1N1) (CA09) [9]. Theoretically, VHH (R1a-G6) functionally blocks attachment of HA to receptors on cell surface which was mediated by the globular

head domain. Here, these data suggested that multimerization of VHH improved the binding affinity and breath of the nanobodies and prolonged the blood half-life *in vivo* in line with published research [39]. It is better structurally identified the epitope recognized by VHH to lay the basis for heterologous protection between VHH and different influeza virus strains. The multimerization of a nanobody, fenobody, is not only superior to that of a monovalent nanobody but also enhances sensitivity and specificity and elongates the half-life *in vivo*. This study may lay a foundation for the establishment of a broad range of neutralizing drugs for the prevention and treatment of influenza viruses. In this study, the limitation is only A/Puerto Rico/8/1934 (H1N1) influenza virus was employed to test the neutralization and protection of ferritin-NP-VHH and monovalent VHH. In the future work, an array of influenza viruses should be used to tested for cross-protection conferred by ferritin-NP-VHH, such as H3N2, H5N1 and H7N9 influenza viruses. In this study, ferritin cage (SpyTag-ferritin) control group is not included in the animal experiments. It is possible that the SpyTag/SpyCatcher components or ferritin cage could induce a non-specific innate immune response that contributes to virus and nanoparticle clearance. It is inevitable to test the innate immunty stimulation by SpyTag/SpyCatcher components or ferritin cage that could limit the repeated administration with SpyTag-ferritin on behalf of the clinical application of fenobody.

Despite these advantages, ferritin is highly conserved from prokaryote to mammal species and has immunogenicity [42]. Challenges still lie in the clinical application of fenobodies, such as possible anti-ferritin antibodies due to repeated administration, safety concern, comparably high production costs, and poor payload delivery performance. However, with the obvious advantages of high stability and biocompatibility, fenobodies are still promising platforms for the development of nanotecnology-based drugs.

5. Conclusions

The ferritin-NP-VHH based on ferritin nanoparticles not only displays the advantages of traditional VHH but also has the advantages of high sensitivity and long half-life. Thus, it is of great significance and potential to the prevention and treatment of infection by influenza A (H1N1) viruses and other subtypes.

Availability of Data and Materials

The data underlying this article are available in the article and are available upon request from corresponding author.

Author Contributions

QWeng and JL designed this research study. QWeng, HL, XY, and CX performed the research and made figures. QWang and YX collected the samples and search references. JL wrote and revised the manuscript. All authors read and approved the final manuscript. All authors contributed to editorial changes in the manuscript. All authors have participated sufficiently in the work and agreed to be accountable for all aspects of the work.

Ethics Approval and Consent to Participate

In this study, the animal experimental protocol was approved by the Institutional Animal Care and Use Committee at Qingdao Agricultural University (approval reference number # 20200018), and animal experiments were conducted at Qingdao Agricultural University. All animal experimental tests were carried out in accordance with the 2016 laboratory animal standards in China and other related regulations in the Animal Welfare Act.

Acknowledgment

We appreciate all the funders for supporting this study. As well, we appreciate Dr. Aidong Gu's advice and suggestion on this study.

Funding

This study was supported by Nanjing Important Science & Technology Specific Projects (2021-11005) and the Innovation Center for Infectious Disease of Jiangsu Province (NO. CXZX202232).

Conflict of Interest

The authors declare no conflict of interest.

References

[1] Dangi T, Jain A. Influenza Virus: A Brief Overview. Proceedings of the National Academy of Sciences, India. Section B. 2012; 82: 111–121. https://doi.org/10.1007/s40011-011-0009-6.

[2] Pleschka S. Overview of influenza viruses. Current Topics in Microbiology and Immunology. 2013; 370: 1–20. https://doi.org/10.1007/82_2012_272.

[3] Rappazzo CG, Watkins HC, Guarino CM, Chau A, Lopez JL, DeLisa MP, *et al*. Recombinant M2e outer membrane vesicle vaccines protect against lethal influenza A challenge in BALB/c mice. Vaccine. 2016; 34: 1252–1258. https://doi.org/10.1016/j.vaccine.2016.01.028.

[4] Han J, Perez J, Schafer A, Cheng H, Peet N, Rong L, *et al*. Influenza Virus: Small Molecule Therapeutics and Mechanisms of Antiviral Resistance. Current Medicinal Chemistry. 2018; 25: 5115–5127. https://doi.org/10.2174/0929867324666170920165926.

[5] Lyons DM, Lauring AS. Mutation and Epistasis in Influenza Virus Evolution. Viruses. 2018; 10: 407. https://doi.org/10.3390/v10080407.

[6] van der Vries E, Schutten M, Fraaij P, Boucher C, Osterhaus A. Influenza virus resistance to antiviral therapy. Advances in Pharmacology (San Diego, Calif.). 2013; 67: 217–246. https://doi.org/10.1016/B978-0-12-405880-4.00006-8.

[7] Yao Y, Wang H, Chen J, Shao Z, He B, Chen J, *et al*. Protection against homo and hetero-subtypic influenza A virus by optimized M2e DNA vaccine. Emerging Microbes & Infec-

tions. 2019; 8: 45–54. https://doi.org/10.1080/22221751.2018.1558962.

[8] Girard MP, Tam JS, Assossou OM, Kieny MP. The 2009 A (H1N1) influenza virus pandemic: A review. Vaccine. 2010; 28: 4895–4902. https://doi.org/10.1016/j.vaccine.2010.05.031.

[9] Hufton SE, Risley P, Ball CR, Major D, Engelhardt OG, Poole S. The breadth of cross sub-type neutralisation activity of a single domain antibody to influenza hemagglutinin can be increased by antibody valency. PloS One. 2014; 9: e103294. https://doi.org/10.1371/journal.pone.0103294.

[10] Hayden FG. Antiviral resistance in influenza viruses–implications for management and pandemic response. The New England Journal of Medicine. 2006; 354: 785–788. https://doi.org/10.1056/NEJMp068030.

[11] Lowen AC, Palese P. Influenza virus transmission: basic science and implications for the use of antiviral drugs during a pandemic. Infectious Disorders Drug Targets. 2007; 7: 318–328. https://doi.org/10.2174/187152607783018736.

[12] Liu Y, Huang H. Expression of single-domain antibody in different systems. Applied Microbiology and Biotechnology. 2018; 102: 539–551. https://doi.org/10.1007/s00253-017-8644-3.

[13] Muyldermans S. Nanobodies: natural single-domain antibodies. Annual Review of Biochemistry. 2013; 82: 775–797. https://doi.org/10.1146/annurev-biochem-063011-092449.

[14] Salvador JP, Vilaplana L, Marco MP. Nanobody: outstanding features for diagnostic and therapeutic applications. Analytical and Bioanalytical Chemistry. 2019; 411: 1703–1713. https://doi.org/10.1007/s00216-019-01633-4.

[15] Akazawa-Ogawa Y, Uegaki K, Hagihara Y. The role of intradomain disulfide bonds in heat-induced irreversible denaturation of camelid single domain VHH antibodies. Journal of Biochemistry. 2016; 159: 111–121. https://doi.org/10.1093/jb/mvv082.

[16] Goldman ER, Liu JL, Zabetakis D, Anderson GP. Enhancing Stability of Camelid and Shark Single Domain Antibodies: An Overview. Frontiers in Immunology. 2017; 8: 865. https://doi.org/10.3389/fimmu.2017.00865.

[17] Liu H, Schittny V, Nash MA. Removal of a Conserved Disulfide Bond Does Not Compromise Mechanical Stability of a VHH Antibody Complex. Nano Letters. 2019; 19: 5524–5529. https://doi.org/10.1021/acs.nanolett.9b02062.

[18] Liu JL, Shriver-Lake LC, Anderson GP, Zabetakis D, Goldman ER. Selection, characterization, and thermal stabilization of llama single domain antibodies towards Ebola virus glycoprotein. Microbial Cell Factories. 2017; 16: 223. https://doi.org/10.1186/s12934-017-0837-z.

[19] Steeland S, Vandenbroucke RE, Libert C. Nanobodies as therapeutics: big opportunities for small antibodies. Drug Discovery Today. 2016; 21: 1076–1113. https://doi.org/10.1016/j.drudis.2016.04.003.

[20] Kalathiya U, Padariya M, Fahraeus R, Chakraborti S, Hupp TR. Multivalent Display of SARS-CoV-2 Spike (RBD Domain) of COVID-19 to Nanomaterial, Protein Ferritin Nanocages. Biomolecules. 2021; 11: 297. https://doi.org/10.3390/biom11020297.

[21] Kanekiyo M, Wei CJ, Yassine HM, McTamney PM, Boyington JC, Whittle JRR, *et al*. Self-assembling influenza nanoparticle vaccines elicit broadly neutralizing H1N1 antibodies. Nature. 2013; 499: 102–106. https://doi.org/10.1038/nature12202.

[22] Yamashita I, Iwahori K, Kumagai S. Ferritin in the field of nanodevices. Biochimica et Biophysica Acta. 2010; 1800: 846–857. https://doi.org/10.1016/j.bbagen.2010.03.005.

[23] Bhushan B, Kumar SU, Matai I, Sachdev A, Dubey P, Gopinath P. Ferritin nanocages: a novel platform for biomedical applications. Journal of Biomedical Nanotechnology. 2014; 10: 2950–2976. https://doi.org/10.1166/jbn.2014.1980.

[24] He J, Fan K, Yan X. Ferritin drug carrier (FDC) for tumor targeting therapy. Journal of Controlled Release: Official Journal of the Controlled Release Society. 2019; 311–312: 288–300. https://doi.org/10.1016/j.jconrel.2019.09.002.

[25] Zang J, Chen H, Zhao G, Wang F, Ren F. Ferritin cage for encapsulation and delivery of bioactive nutrients: From structure, property to applications. Critical Reviews in Food Science and Nutrition. 2017; 57: 3673–3683. https://doi.org/10.1080/10408398.2016.1149690.

[26] Zhang B, Tang G, He J, Yan X, Fan K. Ferritin nanocage: A promising and designable multi-module platform for constructing dynamic nanoassembly-based drug nanocarrier. Advanced Drug Delivery Reviews. 2021; 176: 113892. https://doi.org/10.1016/j.addr.2021.113892.

[27] Liu Z, Zhou H, Wang W, Tan W, Fu YX, Zhu M. A novel method for synthetic vaccine construction based on protein assembly. Scientific Reports. 2014; 4: 7266. https://doi.org/10.1038/srep07266.

[28] Wang W, Liu Z, Zhou X, Guo Z, Zhang J, Zhu P, *et al*. Ferritin nanoparticle-based SpyTag/SpyCatcher-enabled click vaccine for tumor immunotherapy. Nanomedicine: Nanotechnology, Biology, and Medicine. 2019; 16: 69–78. https://doi.org/10.1016/j.nano.2018.11.009.

[29] Wang W, Zhou X, Bian Y, Wang S, Chai Q, Guo Z, *et al*. Dual-targeting nanoparticle vaccine elicits a therapeutic antibody response against chronic hepatitis B. Nature Nanotechnology. 2020; 15: 406–416. https://doi.org/10.1038/s41565-020-0648-y.

[30] Zakeri B, Fierer JO, Celik E, Chittock EC, Schwarz-Linek U, Moy VT, *et al*. Peptide tag forming a rapid covalent bond to a protein, through engineering a bacterial adhesin. Proceedings of the National Academy of Sciences of the United States of America. 2012; 109: E690–E697. https://doi.org/10.1073/pnas.1115485109.

[31] Dahodwala H, Sharfstein ST. The 'Omics Revolution in CHO Biology: Roadmap to Improved CHO Productivity. Methods in Molecular Biology (Clifton, N.J.). 2017; 1603: 153–168. https://doi.org/10.1007/978-1-4939-6972-2_10.

[32] Fischer S, Handrick R, Otte K. The art of CHO cell engineering: A comprehensive retrospect and future perspectives. Biotechnology Advances. 2015; 33: 1878–1896. https://doi.org/10.1016/j.biotechadv.2015.10.015.

[33] Jain NK, Barkowski-Clark S, Altman R, Johnson K, Sun F, Zmuda J, *et al*. A high density CHO-S transient transfection system: Comparison of ExpiCHO and Expi293. Protein Expression and Purification. 2017; 134: 38–46. https://doi.org/10.1016/j.pep.2017.03.018.

[34] Omasa T, Onitsuka M, Kim WD. Cell engineering and cultivation of chinese hamster ovary (CHO) cells. Current Pharmaceutical Biotechnology. 2010; 11: 233–240. https://doi.org/10.2174/138920110791111960.

[35] Reinhart D, Damjanovic L, Kaisermayer C, Sommeregger W, Gili A, Gasselhuber B, *et al*. Bioprocessing of Recombinant CHO-K1, CHO-DG44, and CHO-S: CHO Expression Hosts Favor Either mAb Production or Biomass Synthesis. Biotechnology Journal. 2019; 14: e1700686. https://doi.org/10.1002/biot.201700686.

[36] de Marco A. Recombinant expression of nanobodies and nanobody-derived immunoreagents. Protein Expression and Purification. 2020; 172: 105645. https://doi.org/10.1016/j.pep.2020.105645.

[37] Rossotti MA, Bélanger K, Henry KA, Tanha J. Immunogenicity and humanization of single-domain antibodies. The FEBS Journal. 2022; 289: 4304–4327. https://doi.org/10.1111/febs.15809.

[38] Wang X, Sheng Y, Ji P, Deng Y, Sun Y, Chen Y, *et al*. A Broad-specificity Neutralizing Nanobody against Hepatitis E Virus Capsid Protein. Journal of Immunology (Baltimore, Md.:

1950). 2024; 213: 442–455. https://doi.org/10.4049/jimmunol.2300706.

[39] Fan K, Jiang B, Guan Z, He J, Yang D, Xie N, *et al*. Fenobody: A Ferritin-Displayed Nanobody with High Apparent Affinity and Half-Life Extension. Analytical Chemistry. 2018; 90: 5671–5677. https://doi.org/10.1021/acs.analchem.7b05217.

[40] Zhang W, Wang H, Wu T, Gao X, Shang Y, Zhang Z, *et al*. A SARS-CoV-2 Nanobody Displayed on the Surface of Human Ferritin with High Neutralization Activity. International Journal of Nanomedicine. 2024; 19: 2429–2440. https://doi.org/10.2147/IJN.S450829.

[41] Liao X, Wang J, Guo B, Bai M, Zhang Y, Yu G, *et al*. Enhancing Nanobody Immunoassays through Ferritin Fusion: Construction of a *Salmonella*-Specific Fenobody for Improved Avidity and Sensitivity. Journal of Agricultural and Food Chemistry. 2024; 72: 14967–14974. https://doi.org/10.1021/acs.jafc.4c03606.

[42] Truffi M, Fiandra L, Sorrentino L, Monieri M, Corsi F, Mazzucchelli S. Ferritin nanocages: A biological platform for drug delivery, imaging and theranostics in cancer. Pharmacological Research. 2016; 107: 57–65. https://doi.org/10.1016/j.phrs.2016.03.002.